Low-dimensional magnetic properties of orthorhombic MnV_2O_6: A nonstandard structure stabilized at high pressure

M. L. Hneda,[1,2,3] J. B. M. da Cunha,[1] M. A. Gusmão,[1] S. R. Oliveira Neto,[4,2] J. Rodríguez-Carvajal,[5] and O. Isnard[2,3]

[1]*Instituto de Física, Universidade Federal do Rio Grande do Sul, CP 15051, 91501-970 Porto Alegre, Brazil*

[2]*CNRS, Institut Néel, 71 Avenue des Martys, CS 20156, F-38042 Grenoble, France*

[3]*Université Grenoble Alpes, Institut Néel, F-38042 Grenoble, France*

[4]*Universidade Federal de Sergipe, 49100-000 São Cristóvão, Brazil*

[5]*Institut Laue-Langevin (ILL), 6 Rue Jules Horowitz, BP 156, F-38042 Grenoble, France*

(Received 23 September 2016; published 19 January 2017)

This paper presents the physical properties of a nonstandard orthorhombic form of MnV_2O_6, including a comparison with the isostructural orthorhombic niobate $MnNb_2O_6$, and with the usual MnV_2O_6 monoclinic polymorph. Orthorhombic ($Pbcn$) MnV_2O_6 is obtained under extreme conditions of high pressure (6.7 GPa) and high temperature (800 °C). A negative Curie-Weiss temperature θ_{CW} is observed, implying dominant antiferromagnetic interactions at high temperatures, in contrast to the positive θ_{CW} of the monoclinic form. Specific-heat measurements are reported down to 1.8 K for all three compounds, and corroborate the magnetic-transition temperatures obtained from susceptibility data. Orthorhombic MnV_2O_6 presents a transition to an ordered antiferromagnetic state at $T_N = 4.7$ K. Its magnetic structure, determined by neutron diffraction, is unique among the columbite compounds, being characterized by a commensurate propagation vector $\mathbf{k} = (0,0,\frac{1}{2})$. It presents antiferromagnetic chains running along the c axis, but with a different spin pattern in comparison to the chains observed in $MnNb_2O_6$. By a comparative discussion of our observations in this three compounds, we are able to highlight the interplay between competing interactions and dimensionality that yield their magnetic properties.

DOI: 10.1103/PhysRevB.95.024419

I. INTRODUCTION

When crystallized at ambient pressure, manganese vanadate MnV_2O_6 presents a monoclinic structure, the so-called brannerite, with the space group $C2/m$ [1,2]. This phase is characterized by chains of MnO_6 octahedra along the b axis, connected by parallel chains of VO_6 octahedra [1]. Slightly above 540 °C, this material undergoes a phase transition to a high-temperature pseudobrannerite phase, similar to brannerite but with a "rotation" of $(VO_6)_n$ chains around the b axis, with the oxygen O2 moving away from vanadium, whose coordination becomes a trigonal bipyramid, VO_5 [3].

Under high pressure and high temperature, MnV_2O_6 transforms into an orthorhombic $Pbcn$ crystal structure [4]. This pressure-induced transformation has been reported to involve an increase of vanadium coordination from "5 + 1" to 6, followed by a change in oxygen packing [1]. The resulting structure is the same observed for $MnNb_2O_6$, or, more generally, for ANb_2O_6, with A being typically an iron-group metal. It is characterized by magnetic A^{2+} ions arranged in A-O layers (on the bc plane), separated by two nonmagnetic Nb^{2+} planes along the a axis. This configuration contains weakly interacting magnetic chains [5–8], with the strongest exchange couplings occurring between A ions within each chain [8,9]. Such interesting low-dimensional magnetic properties are one of the main motivations for the present study.

Unlike most of the AB_2O_6 compounds (B = Ta, Nb), which exhibit low-dimensional properties, brannerite MnV_2O_6 is known to be a three-dimensional (3D) antiferromagnet, with a Néel temperature $T_N = 19$ K [1]. For comparison, the magnetic transition of $MnNb_2O_6$ occurs at 4.40 K [10–12]. We have recently reported [8] on a series of isostructural compounds $MnNb_{2-x}V_xO_6$, for $x \leqslant 0.4$, i.e., in the stability range of the $Pbcn$ structure. All the compounds showed quasi-one-dimensional (1D) magnetic behavior. To the best of our knowledge, studies on the magnetic properties of orthorhombic MnV_2O_6 are lacking. In this paper, utilizing powder x-ray and neutron diffraction as well as magnetic and specific-heat measurements, we present a detailed investigation of the low-temperature magnetic properties of this form of MnV_2O_6 synthesized at high pressure. We also present a comparison between the MnV_2O_6 polymorphs and the related orthorhombic compound, $MnNb_2O_6$.

II. EXPERIMENTAL DETAILS

Samples were prepared with appropriate amounts of Mn acetate ($C_4H_6MnO_4 \cdot 4H_2O$) and V_2O_5. The mixture was ground, pressed into pellets, and heat treated at 400, 650, and 725 °C for 12, 16 and 48 h, respectively. All these heat treatments were interspersed with grinding processes. $MnNb_2O_6$ was later subjected to another heat treatment at 1100 °C for 36 h, and MnV_2O_6 at 725 °C for 48 h. The lower temperature of this latter heat treatment was necessary to avoid evaporation of the precursor, V_2O_5. This was done to ensure a unique phase, and immediately followed by a quenching process. After this treatment, the MnV_2O_6 sample presented a monoclinic structure. This sample was then submitted to a high-temperature high-pressure process, 6.7 GPa at 800 °C for 1 h, in a belt-type press at the Néel Institut in Grenoble.

The sample purity was checked by an x-ray diffraction (XRD) analysis, followed by neutron diffraction (ND). The XRD was performed in Bragg-Brentano geometry, using Cu $K\alpha$ radiation, with a scan step of 0.05°, and an angular 2θ range from 10° to 90°. ND patterns were recorded with

the double-axis high-flux diffractometer D1B operated by the CNRS at the Institut Laue-Langevin (ILL), Grenoble, using a 2.52 Å wavelength selected by a pyrolytic graphite monochromator. D1B is a powder diffractometer operating with a monochromator take-off angle of 44° (in 2θ). In this configuration the multicounter is composed of 1280 cells, covering a total angular (2θ) range of 128°, in detector steps of 0.1°. A vanadium sample holder was used. A Rietveld refinement with the FULLPROF suite package [13] was performed for XRD and ND data to extract the crystallographic and magnetic parameters. Agreement factors used in this paper are defined according to the guidelines of the Rietveld refinement [14].

Magnetic properties were measured on powder samples, in the temperature range from 1.6 to 300 K, using an extraction magnetometer. Specific-heat measurements were performed on pellets (mass ∼5 mg) using the temperature-relaxation method, which consists of increasing the sample temperature with a known power, then fitting the temperature relaxation during heating and cooling. Measurements were carried out in the range of 1.8–300 K, using a physical property measurement system (PPMS, Quantum Design).

III. RESULTS AND DISCUSSION

A. X-ray diffraction

Sample synthesis began from the standard monoclinic material obtained at ambient pressure. Then, after the high-pressure and high-temperature treatment, MnV_2O_6 presented an orthorhombic *Pbcn* space-group symmetry. Figure 1 shows a Rietveld analysis of the XRD pattern recorded at room temperature for the orthorhombic form. Table I shows the obtained parameters: atomic positions, cell parameters, and agreement factors R_{WP} and R_B of the Rietveld refinement. The unit-cell parameters are practically identical to those published by Gondrand *et al.* [4]. The corresponding values for the isostructural compound $MnNb_2O_6$ are also given for comparison in Table I. MnV_2O_6 has a cell volume 11% smaller

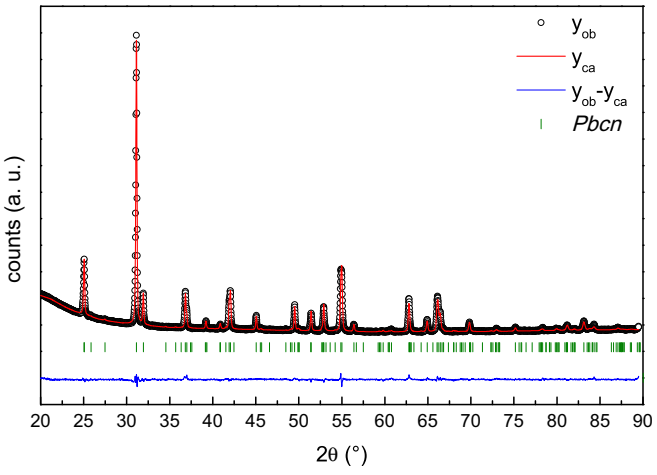

FIG. 1. Rietveld refinement of the x-ray diffraction (λ = 1.540 Å) pattern recorded at room temperature for orthorhombic MnV_2O_6 obtained at high pressure. The Bragg positions at the bottom correspond to the *Pbcn* space group, as indicated.

TABLE I. Structural parameters obtained at room temperature from a Rietveld refinement of the XRD pattern for MnV_2O_6 compared to that of $MnNb_2O_6$ [8], both orthorhombic *Pbcn* compounds.

		$MnNb_2O_6$	MnV_2O_6
Mn	x	0	0
	y	0.180(3)	0.196(1)
	z	0.25	0.25
Nb/V	x	0.1626(3)	0.1698(4)
	y	0.3188(9)	0.3202(9)
	z	0.760(2)	0.753(2)
O1	x	0.102(2)	0.0967(6)
	y	0.412(5)	0.413(2)
	z	0.445(7)	0.434(3)
O2	x	0.083(2)	0.0996(8)
	y	0.127(6)	0.148(2)
	z	0.888(7)	0.863(3)
O3	x	0.253(3)	0.263(1)
	y	0.127(6)	0.120(3)
	z	0.586(6)	0.597(5)
a (Å)		14.431(1)	13.7722(7)
b (Å)		5.7638(4)	5.6004(3)
c (Å)		5.0820(4)	4.8779(3)
Volume (Å^3)		422.73(5)	376.24(4)
R_{WP} (%)		15.2	8.1
R_B (%)		4.8	6.6

than that of $MnNb_2O_6$, with reductions of 4.6%, 2.8%, and 4.0% for the a, b, and c lattice constants, respectively.

B. Magnetic measurements

The dc susceptibility of MnV_2O_6 samples, both orthorhombic and monoclinic, was recorded as a function of temperature with $\mu_0 H = 0.5$ T. Results are plotted in Fig. 2(a). An expanded view near the low-temperature peaks is shown in the plot inset, showing that these peaks are rather broad, a typical feature of low-dimensional magnetism. In such a case, the Néel temperature corresponds to an inflection point slightly below the maximum [15]. The monoclinic sample shows a transition at $T_N = 19$ K. This is in fair agreement with the value of 20 K reported by Kimber and Attfield [1], while Chuan-Cang *et al.* [2] obtained 17 K. In contrast, we observe a much reduced transition temperature, $T_N = 4.7$ K, in the orthorhombic phase. This temperature is very close to the corresponding one for $MnNb_2O_6$, 4.7 K. In fact, as shown in Fig. 2(b), the susceptibilities of these two *Pbcn* compounds are very close throughout the whole temperature range, despite non-negligible differences in the unit-cell parameters (see Table I).

The paramagnetic susceptibility was fitted to the Curie-Weiss law, $\chi(T) = C/(T - \theta_{CW})$, for temperatures well above T_N. Table II shows the fitted parameters, including a high-temperature effective magnetic moment derived from the Curie constant C. In MnV_2O_6, Mn^{2+} cations are in the $^6S_{5/2}$ electronic state. The appropriate expression for the magnetic moment, $\mu_{\text{eff}} = g\mu_B[S(S+1)]^{1/2}$ [10], gives us $g = 2.1$,

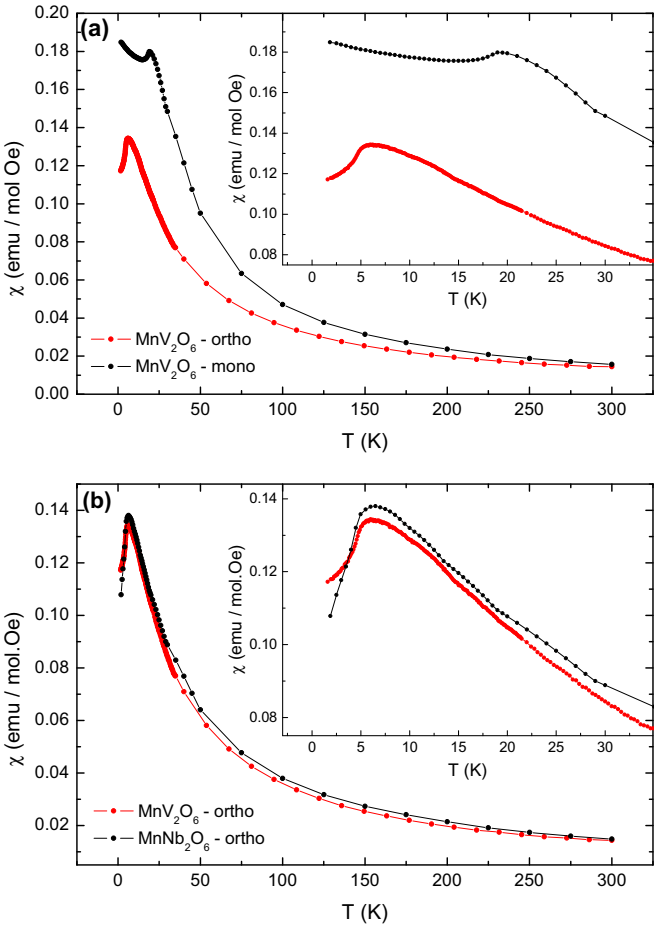

FIG. 2. Comparison of temperature dependence of the dc susceptibility recorded at $\mu_0 H = 0.5$ T for (a) MnV_2O_6 polymorphs, and (b) *Pbcn* isostructural MnV_2O_6 and $MnNb_2O_6$ compounds.

which indicates almost negligible second-order orbital effects. This also means that no significant spin anisotropy should be expected, in contrast to the Ising-like behavior previously observed in other columbites such as (Co/Fe)Nb_2O_6 [16,17]. Curie-Weiss temperatures are negative, again very similar for the vanadium and niobium orthorhombic compounds, and quite large in absolute values, $\theta_{CW} = -24.6$ K for MnV_2O_6 and -24.5 K for $MnNb_2O_6$. In contrast, the monoclinic form of MnV_2O_6 presents a positive $\theta_{CW} = 0.9$ K, which is lower than the values reported in the literature ($\theta_{CW} \simeq 5$ K [1,2]), but still

TABLE II. Néel temperature, Curie-Weiss temperature, Curie constant, effective magnetic moment, and frustration index of MnB_2O_6 samples (B = Nb, V), obtained from measurements of dc susceptibility.

	MnV_2O_6 (monocl.)	MnV_2O_6 (ortho.)	$MnNb_2O_6$ (ortho.)
T_N (K)	19	4.7	4.4
θ_{CW} (K)	0.9	−24.6	−24.5
C (emu K/mol Oe)	4.7	4.46	4.78
μ_{eff} (μ_B)	6.1	6.0	6.2
f		5.2	5.6

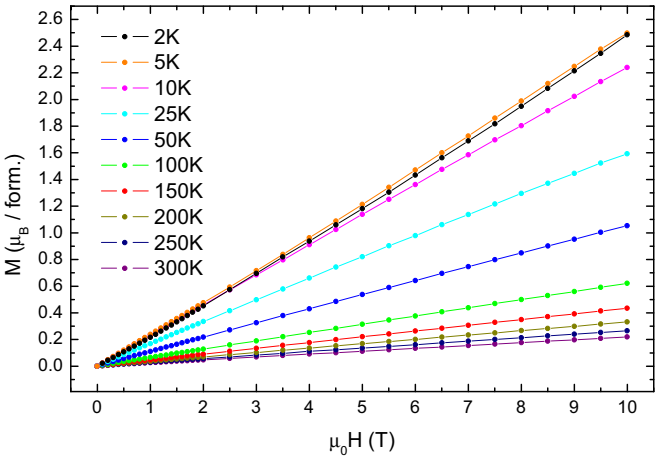

FIG. 3. Isothermal magnetization curves recorded at the indicated temperatures for the orthorhombic form of MnV_2O_6.

positive. We thus see that the dominant exchange interactions in the paramagnetic phase are respectively antiferromagnetic and ferromagnetic for the orthorhombic and monoclinic forms of MnV_2O_6, highlighting the importance of the crystal structure in determining such interactions.

Table II also lists the so-called "frustration index," defined as $f = |\theta_{CW}|/T_N$. It is usual to consider that, for f values around 5 or larger, the system can be considered frustrated [18]. The possibility of having some kind of frustration in the compounds under analysis here will be discussed later on.

To complete this analysis of magnetic properties, isothermal magnetization curves for the orthorhombic MnV_2O_6 compound are shown in Fig. 3 at various temperatures. Their behavior is typical of isotropic antiferromagnetism, in contrast to other ANb_2O_6 orthorhombic systems (A = Fe, Ni), which present Ising-like ferromagnetic chains, and show spin-flip transitions [16,19] in the ordered phase.

C. Specific-heat measurements

The magnetic transition of orthorhombic MnV_2O_6 at low temperatures was also checked through specific-heat measurements. Figure 4 shows specific-heat (C_P) curves in a low-temperature region down to 1.8 K. Magnetic transitions are marked by lambda-shaped peaks, yielding T_N values that agree with those from magnetic measurements (shown in Table II). As seen above with $\chi(T)$, the importance of the crystal structure is put into evidence by the $C_P(T)$ behavior. A close similarity is observed between the orthorhombic compounds MnV_2O_6 and $MnNb_2O_6$, in striking difference with the monoclinic form of MnV_2O_6.

D. Neutron diffraction

Neutron-diffraction measurements were carried out on the orthorhombic MnV_2O_6 sample at 1.5 and 20 K, i.e., below and above the ordering temperature of 4.7 K. The Rietveld refinement of the low-temperature ND pattern ($\lambda = 2.52$ Å) is shown in Fig. 5. The first row of markers below the plot corresponds to Bragg positions of the *Pbcn* ($P\ 2_1/b\ 2/c\ 2_1/n$) space group, and the second one to the magnetic phase

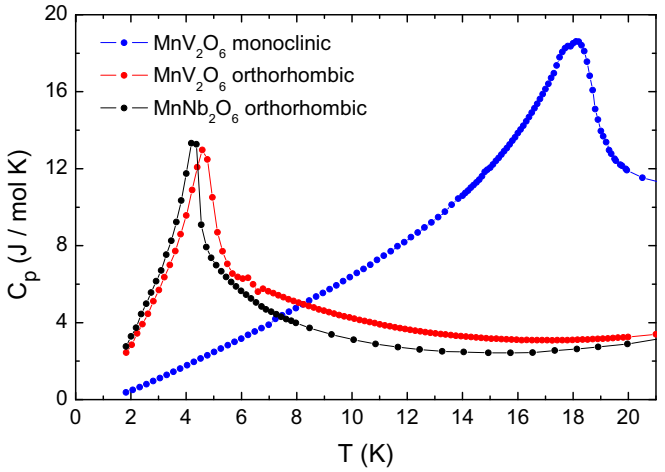

FIG. 4. Low-temperature specific heat of orthorhombic MnV_2O_6 in comparison to its monoclinic polymorph, and with $MnNb_2O_6$.

(indicated as *mag*). As ND is more sensitive to light atoms such as oxygen, this refinement confirms that the oxygen octahedra are packed according to the *Pbcn* crystal symmetry. Due to the almost null neutron coherent-scattering factor of the vanadium atom, its atomic-position parameters were constrained to those derived from XRD. An ND pattern was also recorded at 20 K (not shown in Fig. 5). Table III summarizes the structural parameters obtained from the Rietveld refinements at both 20 and 1.5 K.

The crystal structure of orthorhombic MnV_2O_6, highlighting zigzag chains that run along the c axis, is shown in Fig. 6. These chains are formed by oxygen octahedra surrounding the Mn atoms. Our determination of the magnetic structure from the neutron data is discussed in detail in the Appendix. As a result, at 1.5 K we observe a magnetic order commensurate with the lattice, presenting a propagation vector $\mathbf{k} = (0,0,\frac{1}{2})$. In this configuration, magnetic moments lie essentially on the bc plane, forming a "$++--$" sequence along the chains, with the closest moments on nearest-neighbor chains oriented antiparallel to each other. Such a magnetic structure has

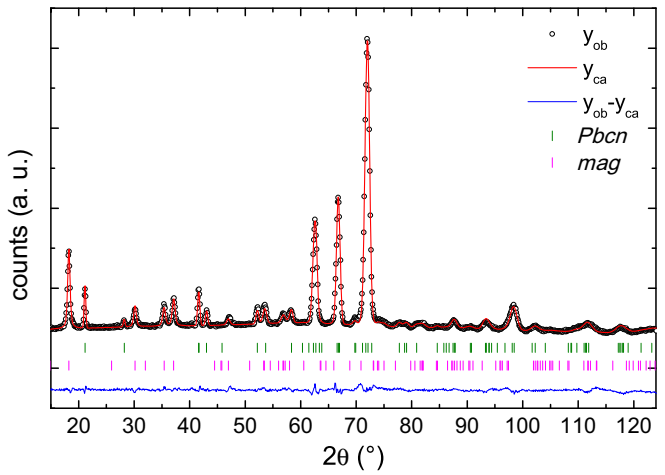

FIG. 5. Rietveld refinement of the ND pattern recorded at 1.5 K for MnV_2O_6, showing structural and magnetic Bragg positions.

TABLE III. Structural, magnetic, and fitting-quality parameters obtained from Rietveld refinement of the ND pattern recorded at the indicated temperatures for orthorhombic MnV_2O_6.

Temp. →		20 K	1.5 K
Mn	x	0.	0.
	y	0.170(6)	0.183(4)
	z	0.25	0.25
V	x	0.1698	0.1698
	y	0.3202	0.3202
	z	0.753	0.753
O1	x	0.095(1)	0.0947(9)
	y	0.403(3)	0.400(2)
	z	0.465(3)	0.462(2)
O2	x	0.087(1)	0.0875(9)
	y	0.109(3)	0.112(2)
	z	0.895(3)	0.895(2)
O3	x	0.255(1)	0.2560(9)
	y	0.143(3)	0.140(2)
	z	0.605(4)	0.607(3)
a (Å)		13.761(4)	13.7580(8)
b (Å)		5.589(2)	5.5889(4)
c (Å)		4.881(2)	4.8805(4)
Volume (Å^3)		375.4(2)	375.28(5)
θ (deg)			82.8
φ (deg)			57.9
μ_{Mn} (μ_B)			3.76(5)
R_{WP} (%)		4.0	2.7
R_B (%)		9.3	5.6
R_M (%)			12.7

yet to be reported in any other columbite compound. In particular, it differs from that of $MnNb_2O_6$, which exhibits antiferromagnetic (AF) zigzag chains forming a "$+-+-$" spin sequence along the c axis [8].

Figure 7 presents the temperature dependence of the Mn magnetic moment in orthorhombic MnV_2O_6, obtained from ND measurements. At 1.5 K, the observed magnetic moment

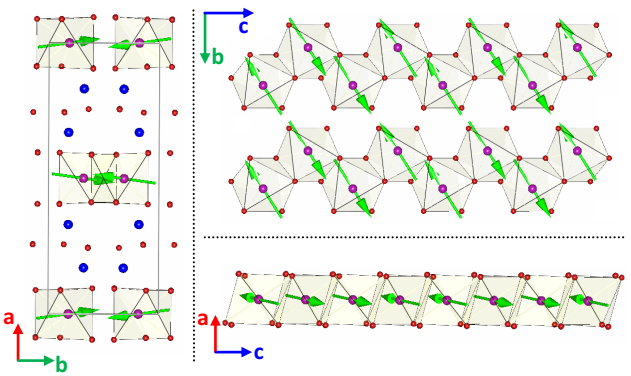

FIG. 6. Three views of the crystal structure of MnV_2O_6 orthorhombic compound, with special focus on the zigzag chains formed by oxygen (red spheres) octahedra surrounding the Mn (pink spheres) atoms along the c axis. Vanadium is shown as blue spheres.

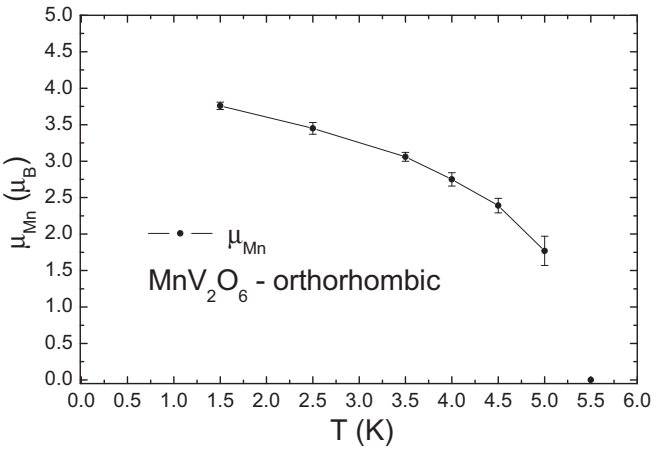

FIG. 7. Temperature dependence of the Mn magnetic moment for MnV_2O_6 as obtained from a Rietveld refinement of the ND patterns. The zero-magnetic-moment result at 5.5 K confirms the absence of long-range order at this temperature.

of Mn^{2+} is $3.76(5)\mu_B$. This value is lower than the spin-only magnetic moment ($5\mu_B$), which may be due to some covalence that is typical in insulating oxides [1]. The zero-moment point in Fig. 7 corresponds to an ND pattern recorded at 5.5 K, which shows no peak related to the magnetic structure, confirming that the system is paramagnetic at that temperature.

E. Discussion

Different magnetic behaviors have been observed here for two MnV_2O_6 polymorphs, which most probably are due to their different crystal structures. Reasoning in this direction, we will develop arguments that help us understand these differences. In the monoclinic form, a Mn^{2+} cation is located at the center of a compressed octahedron, with four oxygens at 2.195 Å on a plane, and two shorter bonds (1.992 Å) to the apical O^{2-} ions. The orthorhombic phase shows a less symmetric Mn environment, in which three pairs of Mn-O distances are observed (2.021, 2.348, and 2.426 Å) so that the mean Mn-O distance changes from 2.127 to 2.265 Å between the $C2/m$ and $Pbcn$ crystal structures. On the other hand, these pairs of oxygen neighbors do not yield a net anisotropy, while the axially compressed octahedron does lead to an easy axis in monoclinic MnV_2O_6 [20]. This helps one to understand why the Néel temperatures are so different, since an Ising-like system can order in two dimensions, but a Heisenberg one must involve interplane interactions. Here, again, there is an important structural difference: The lattice parameter a (interplane direction) has values near 9.3 Å in the monoclinic form and 13.7 Å in the orthorhombic one. Hence, the interplane interactions, ultimately responsible for stabilizing magnetic order, should be weaker in the latter.

The orthorhombic variant features zigzag chains of MnO_6 edge-sharing octahedra running along the c axis. Superexchange occurs through Mn-O-Mn bonds making angles of 86.8°. Actually, there are two such bonds, through two oxygens at the vertices of a shared edge. According to the Goudenough-Kanamori rules [21], such near-90° bond angles should yield (weak) ferromagnetic (FM) superexchange within a chain, involving t_{2g} orbitals. These bond angles are slightly larger in the brannerite, but still closer to 90° than to 180°. So, FM couplings along the chains, although weak, could be dominant, explaining the positive Curie-Weiss temperature. In contrast, the larger and negative values of θ_{CW} observed in the columbite compounds (with V or Nb) seem to be due to interchain AF couplings, possibly a direct Mn-Mn exchange through e_g orbitals. This is consistent with the in-plane order observed in Fig. 6. Nevertheless, such a planar structure can only be stabilized through interplane coupling, as we mentioned before. Since T_N is substantially smaller than θ_{CW}, we have a large frustration index, as indicated in Table II. However, there is no geometric frustration here, in contrast to what was observed for columbites [16,19] with antiferromagnetically coupled FM Ising chains. In the present case, a low T_N arises from the (quasi)low dimensionality and isotropy of the spin system, which can only order in three dimensions, so that the scale of T_N is determined by the weakest exchange interaction.

IV. CONCLUSIONS

We report an investigation of the physical properties of MnV_2O_6 in the columbite crystal structure, with $Pbcn$ symmetry, obtained after a high-temperature and high-pressure treatment of brannerite MnV_2O_6, with the space group $C2/m$.

Both polymorphs share some common features: chains of edge-sharing oxygen octahedra along the c (or b) axis, with a Mn ion at the center of each octahedron; a parallel arrangement of these chains on the bc plane; and weak interplane coupling along the a axis, through layers containing the V ions. But the orientation of the octahedra changes in such a way that there are straight rutile-type MnO_6 chains in the monoclinic form against the zigzag ones in the orthorhombic. Then, subtle differences in the competing exchange interactions lead to quite distinct magnetic behaviors. For instance, the competition between FM intrachain and AF interchain coupling on each magnetic layer yields a spin sequence "$++--$" in the columbite form below T_N, so that the planar spin pattern is as depicted in Fig. 6. In contrast, brannerite MnV_2O_6 was reported to present AF-ordered FM chains [1]. In both cases, since no significant magnetic anisotropy is seen, magnetic ordering is ultimately 3D, stabilized by interplane coupling. In this context, the relatively large difference in T_N (19 K for the brannerite, 4.7 K for the columbite) can be consistently correlated to the interplane distances in these compounds. On the other hand, at high temperatures the net exchange interactions end up being dominated by weak intrachain FM coupling in the monoclinic compound, yielding a small positive Curie-Weiss temperature, while interchain AF coupling is seen to be more important in the orthorhombic one, which shows a large negative θ_{CW}.

It is worth remarking that the relevance of the lattice structure is confirmed by the very similar magnetic properties of the columbite MnV_2O_6 and the isostructural $MnNb_2O_6$, with only small quantitative differences that may be explained by different unit-cell parameters. However, even though the transition temperatures are almost coincident, the intrachain ordering is not the same, with the Nb compound showing a simple alternating sequence "$+-+-$" [8].

TABLE IV. Symmetry operators of the representative cosets of the group BNS P_a2_1/c-I (14.80) in the OG $P_{2a}2_1/c$ (14.6.91) nonstandard setting related to the basis of the paramagnetic group $Pbcn1'$. The symbols (u,v,w) may be interpreted as components of the magnetic moments or as rotation matrices to be applied to the first-atom moment.

First block: (0,0,0)		
No. 1	$(x,y,z;u,v,w)$	$+1$
No. 2	$(-x+\frac{1}{2},y+\frac{1}{2},z;u,-v,-w)$	$+1$
No. 3	$(x+\frac{1}{2},-y+\frac{1}{2},-z;u,-v,-w)$	$+1$
No. 4	$(-x,-y,-z;u,v,w)$	$+1$
Second block: $(0,0,1)'$		
No. 5	$(x,y,z+1;-u,-v,-w)$	-1
No. 6	$(-x+\frac{1}{2},y+\frac{1}{2},z+1;-u,v,w)$	-1
No. 7	$(x+\frac{1}{2},-y+\frac{1}{2},-z+1;-u,v,w)$	-1
No. 8	$(-x,-y,-z+1;-u,-v,-w)$	-1

In conclusion, this study reveals an antiferromagnetic Heisenberg system, MnV_2O_6 in the columbite form. A comparison with its brannerite polymorph and with $MnNb_2O_6$, another columbite compound involving the same cation, puts into evidence the interplay between competing exchange interactions and low-dimensionality effects in determining the magnetic properties of this class of systems.

ACKNOWLEDGMENTS

The authors would like to thank C. Darie, C. Goujon, and M. Legendre for interesting discussions, and help with sample synthesis. Funding for this project was provided by a grant from Région Rhône-Alpes (MIRA scholarship). The present work was also supported in part by the Brazilian agency Conselho Nacional de Desenvolvimento Científico e Tecnológico and by the Brazilian-France agreement CAPES-COFECUB (No. 600/08).

APPENDIX: MAGNETIC STRUCTURE DETERMINATION

In order to determine the propagation vector **k**, we used the software K-SEARCH, which is part of the FULLPROF package [13]. Using BASIREPS (also part of FULLPROF) we found two two-dimensional irreducible representations of $G_{\mathbf{k}} = Pbcn$, giving rise to many solutions of different symmetries for the possible magnetic structures. We then explored the maximal magnetic Shubnikov groups compatible with the propagation vector $\mathbf{k} = (0,0,\frac{1}{2})$. With the information on crystal structure, space group, and propagation vector, we used the program MAXMAGN, from the Bilbao Crystallographic Server [22], which gave us four maximal magnetic groups enabling a nonzero magnetic moment. These four groups [in the standard setting with Belov-Neronova-Smirnova (BNS) notation] are P_annn2, P_anc2, P_a2_1/c-I, and P_a2_1/c-II. Descriptions I and II have different origins (center of symmetry) with respect to the parent paramagnetic group $Pbcn1'$, and a different orientation of the magnetic unit cell with respect to that of the paramagnetic group. None of the orthorhombic magnetic groups provided a solution for the magnetic structure. We obtained that a magnetic structure corresponding to the group P_a2_1/c-I is the only one that fits very well the experimental data.

TABLE V. Sequence of Mn atomic positions ($y = 0.183$) and magnetic-moment components for the magnetic groups BNS P_a2_1/c (I and II) in the setting of the original crystallographic cell of the paramagnetic group $Pbcn1'$.

Mn position	P_a2_1/c-I	P_a2_1/c-II
$(0,y,\frac{1}{4})$	m_x,m_y,m_z	m_x,m_y,m_z
$(\frac{1}{2},y+\frac{1}{2},\frac{1}{4})$	$m_x,-m_y,-m_z$	$-m_x,m_y,m_z$
$(\frac{1}{2},-y+\frac{1}{2},-\frac{1}{4})$	$m_x,-m_y,-m_z$	$m_x,-m_y,-m_z$
$(0,-y,-\frac{1}{4})$	m_x,m_y,m_z	$-m_x,-m_y,-m_z$

A list of symmetry operators of the P_a2_1/c-I group in the nonstandard setting of the parent paramagnetic group $Pbcn1'$ is provided in Table IV, using the Opechowski-Guccione notation (OG), best adapted to the propagation-vector formalism. The first block lists operators strictly necessary to describe the magnetic structure, not associated with time reversal ($+1$ symbol). The second block corresponds to the antitranslation $(0,0,1)'$, associated with time reversal (-1 symbol), which plays the same role as the propagation vector $\mathbf{k} = (0,0,\frac{1}{2})$.

The transformation from the standard setting to the setting used here is $(b,-c,-a;0,0,0)$. The special position of Mn in the paramagnetic space group $Pbcn1'$ becomes a general position in the P_a2_1/c group. Since the OG notation always uses the crystallographic-cell basis, Mn coordinates in this setting are $(0,y,\frac{1}{4})$ with $y \sim 0.183$, identical to those in $Pbcn$. There is no constraint on magnetic-moment orientation for the first representative Mn atom. Both monoclinic descriptions display a different sequence of magnetic-moment components in the parent-group basis, and only the sequence of group BNS P_a2_1/c agrees with the experimental data. This is shown in Table V.

[1] S. A. J. Kimber and J. P. Attfield, Disrupted antiferromagnetism in the brannerite MnV_2O_6, Phys. Rev. B **75**, 064406 (2007).

[2] Z. Chuan-Cang, L. Fa-Min, D. Peng, C. Lu-Gang, Z. Wen-Wu, and Z. Huan, Synthesis, structure and antiferromagnetic behavior of brannerite MnV_2O_6, Chin. Phys. B **19**, 067503 (2010).

[3] K. Mocala and J. Ziólkowski, Polymorphism of the bivalent metal vanadates MeV_2O_6 (Me = Mg, Ca, Mn, Co, Ni, Cu, Zn, Cd), J. Solid State Chem. **69**, 299 (1987).

[4] M. Gondrand, A. Collomb, J. C. Joubert, and R. D. Shannon, Synthesis of new high-pressure columbite phases containing pentavalent vanadium, J. Solid State Chem. **11**, 1 (1974).

[5] C. Heid, H. Weitzel, P. Burlet, M. Bonnet, W. Gonschorek, T. Vogt, J. Norwig, and H. Fuess, Magnetic phase diagram of $CoNb_2O_6$: A neutron diffraction study, J. Magn. Magn. Mater. **151**, 123 (1995).

[6] S. Kobayashi, S. Mitsuda, M. Ishikawa, K. Miyatani, and K. Kohn, Three-dimensional magnetic ordering in the quasi-one-dimensional Ising magnet $CoNb_2O_6$ with partially released geometrical frustration, Phys. Rev. B **60**, 3331 (1999).

[7] C. Heid, H. Weitzel, P. Burlet, M. Winkelmann, H. Ehrenberg, and H. Fuess, Magnetic phase diagrams of $CoNb_2O_6$, Physica B **234-236**, 574 (1997).

[8] M. L. Hneda, J. B. M. da Cunha, M. A. C. Gusmão, and O. Isnard, Low dimensional magnetism in $MnNb_{2-x}V_xO_6$, Mater. Res. Bull. **74**, 169 (2016).

[9] I. Maartense and I. Yaeger, Field-induced magnetic transitions of $CoNb_2O_6$ in the ordered state, Solid State Commun. **21**, 93 (1977).

[10] O. V. Nielsen, B. Lebech, F. Krebs Larsen, L. M. Holmes, and A. A. Ballman, A neutron diffraction study of the nuclear and magnetic structure of $MnNb_2O_6$, J. Phys. C **9**, 2401 (1976).

[11] L. M. Holmes, A. A. Ballman, and R. R. Hecker, Antiferromagnetic ordering in $MnNb_2O_6$ studied by magnetoelectric and magnetic susceptibility measurements, Solid State Commun. **11**, 409 (1972).

[12] D. Prabhakaran, F. R. Wondre, and A. T. Boothroyd, Preparation of large single crystals of ANb_2O_6 (A = Ni, Co, Fe, Mn) by the floating-zone method, J. Cryst. Growth **250**, 72 (2003).

[13] J. Rodriguez-Carvajal, Recent advances in magnetic structure determination by neutron powder diffraction, Physica B **192**, 55 (1993).

[14] L. B. McCusker, R. B. Von Dreele, D. E. Cox, D. Louer, and P. Scardi, Rietveld refinement guidelines, J. Appl. Crystallogr. **32**, 36 (1999).

[15] L. J. de Jongh and A. R. Miedema, Experiments on simple magnetic model systems, Adv. Phys. **23**, 1 (1974).

[16] P. W. C. Sarvezuk, M. A. Gusmão, J. B. M. da Cunha, and O. Isnard, Magnetic behavior of the $Ni_xFe_{1x}Nb_2O_6$ quasi-one-dimensional system: Isolation of Ising chains by frustration, Phys. Rev. B **86**, 054435 (2012).

[17] P. W. C. Sarvezuk, E. J. Kinast, C. V. Colin, M. A. Gusmão, J. B. M. da Cunha, and O. Isnard, New investigation of the magnetic structure of $CoNb_2O_6$ columbite, J. Appl. Phys. **109**, 07E160 (2011).

[18] A. P. Ramirez, Strongly geometrically frustrated magnets, Annu. Rev. Mater. Sci. **24**, 453 (1994).

[19] P. W. C. Sarvezuk, E. J. Kinast, C. V. Colin, M. A. Gusmão, J. B. M. da Cunha, and O. Isnard, Suppression of magnetic ordering in quasi-one-dimensional $Fe_xCo_{1x}Nb_2O_6$ compounds, Phys. Rev. B **83**, 174412 (2011).

[20] S.-Y. Park, Y.-H. Jeong, and T.-Y. Koo, Field-induced spin-flop transition in a one-dimensional chain of MnV_2O_6, J. Korean Phys. Soc. **64**, 710 (2014).

[21] J. B. Goodenough, *Magnetism and the Chemical Bond* (Interscience, New York, 1963).

[22] J. M. Perez-Mato, S. V. Gallego, E. S. Tasci, L. Elcoro, G. de la Flor, and M. I. Aroyo, Symmetry-based computational tools for magnetic crystallography, Annu. Rev. Mater. Res. **45**, 217 (2015).